G Model
APSUSC-33792; No. of Pages 4
ARTICLE IN PRESS
Applied Surface Science xxx (2016) xxx–xxx
Contents lists available at ScienceDirect
Applied Surface Science
journal homepage: www.elsevier.com/locate/apsusc

Superconductor-ferromagnet-superconductor nanojunctions from perovskite materials

V. Štrbík [a,*], Š. Beňačka [a], Š. Gaži [a], M. Španková [a], V. Šmatko [a], J. Knoška [b,c], N. Gál [a], Š. Chromik [a], M. Sojková [a], M. Pisarčík [a]

[a] Institute of Electrical Engineering, SAS, Dúbravská Cesta 9, Bratislava, Slovakia
[b] Center for Free-Electron Laser Science, DESY, Notkestraβe 85, 22607, Hamburg, Germany
[c] Department of Physics, University of Hamburg, Luruper Chaussee 149, 22607, Hamburg, Germany

ARTICLE INFO

Article history:
Received 29 February 2016
Received in revised form 19 July 2016
Accepted 8 August 2016
Available online xxx

Keywords:
Superconductor-ferromagnet-superconductor
nanojunction
Triplet superconductivity
Perovskite materials

ABSTRACT

The lateral superconductor-ferromagnet–superconductor (SFS) nanojunctions based on high critical temperature superconductor $YBa_2Cu_3O_x$ (YBCO) and half-metallic ferromagnet $La_{0.67}Sr_{0.33}MnO_3$ (LSMO) thin films were prepared to investigate a possible presence of long range triplet component (LRTC) of Cooper pairs in the LSMO. We applied Ga^{3+} focused ion beam patterning to create YBCO/LSMO/YBCO lateral type nanojunctions with LSMO length as small as 40 nm. The resistivity vs. temperature, critical current density vs. temperature and resistance vs. magnetic field dependence were studied to recognize the LRTC of Cooper pairs in the LSMO. A non-monotonic temperature dependence of junction critical current density and a decrease of the SFS nanojunction resistance in increased magnetic field were observed. Only weak manifestations of LRTC and some qualitative agreement with theory were found out in SFS nanojunctions realized from the perovskite materials. The presence of equal-spin triplet component of Cooper pairs in half-metallic LSMO ferromagnet is not such apparent as in SFS junctions prepared from low temperature superconductors NbTiN and half-metallic ferromagnet CrO_2.

1. Introduction

Metallic ferromagnet (F), in proximity with a superconductor (S), can transport supercurrent on long distance through conversion of opposite-spin singlet Cooper pairs (CP) into equal-spin triplet CP [1]. Theoretical and experimental studies of equal spin long-range triplet component (LRTC) in superconductor-ferromagnet (SF) proximity heterostructures demonstrate, besides new physical aspects, application possibilities for spintronics, superconducting quantum interference devices and Josephson junctions operating in strong magnetic fields [2]. The penetration depth of CP into a diffusive normal metal (N) is given by the coherence length $\xi_N = (\hbar D_N/2\pi k_B T)^{1/2}$, achieving 1 μm at very low temperature, whereas ferromagnet exchange energy $E_{ex} \gg k_B T$ makes the penetration depth in diffusive ferromagnet much shorter $\xi_F = (\hbar D_F/2\pi E_{ex})^{1/2} \approx 1$ nm, here T is temperature, $D_F = v_F l_F/3$ diffusion constant, v_F the Fermi velocity of carriers, l_F the mean free path and $\hbar$ and k_B are the Planck and Boltzmann constants. However, at convenient conditions (magnetic inhomogeneity, spin active SF interface) the conversion of spin singlet CP into the LRTC can enhance ξ_F close to ξ_N. The LRTC as a Josephson supercurrent through the strong half-metallic CrO_2 has been recently observed using low temperature NbTiN superconductor [3] or Nb with various ferromagnetic barrier (Ni, Fe, Co, Cr)[4–6]. The realization of high-quality SF structures or SFS Josephson weak links based on high temperature superconductor $YBa_2Cu_3O_x$ (YBCO) and structurally compatible half-metallic $La_{0.67}Sr_{0.33}MnO_3$ (LSMO), is a very complicated task for manifesting the LRTC. Kasai et al. [7] presented the supercurrent in YBCO/$La_{0.7}Ca_{0.3}MnO_x$/YBCO stack type junctions (current transport in c-axis direction) which was ascribed to novel mechanism of proximity effect. The thicknesses of all layers were 200 nm. The superconductor $Pr_{1.85}Ce_{0.15}CuO_{4-\delta}$ (PCCO) with a critical temperature of about 15 K was used in PCCO(250 nm)/LCMO(5–65 nm)/PCCO(250 nm) stack junctions [8]. The superconducting properties of junctions were presented at very low temperatures (2 K) and were ascribed to long range proximity effect. The junction parameters such as the transparency of the SF interface, the greatness of the exchange energy E_{ex}, the ferromagnet resistivity, the geometry of junction and coherence length of high temperature superconductor play a crucial role in conversion from spin singlet to spin triplet CP. To increase the presence of LRTC in SFS heterostructure the magnetic inhomogeneity and lat-

* Corresponding author.
E-mail address: vladimir.strbik@savba.sk (V. Štrbík).

http://dx.doi.org/10.1016/j.apsusc.2016.08.044
0169-4332/

Please cite this article in press as: V. Štrbík, et al., Superconductor-ferromagnet-superconductor nanojunctions from perovskite materials, Appl. Surf. Sci. (2016), http://dx.doi.org/10.1016/j.apsusc.2016.08.044

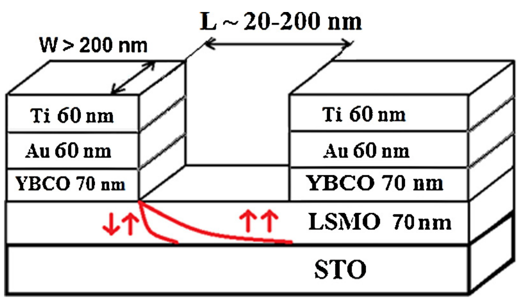

Fig. 1. Sketch of the YBCO/LSMO/YBCO nanojunction of lateral geometry. The length L of the LSMO between the YBCO thin films was set up by parallel incidence of gallium focused ion beam.

eral geometry should be more convenient, as showed theoretical investigations [9].

In this paper we report the preparation and study of LSMO/YBCO bilayers and nanometer sized YBCO/LSMO/YBCO heterostructures of lateral geometry using Ga^{3+} focused ion beam (FIB) patterning to clear up whether this approach is a suitable tool for the preparation of SFS nanojunctions in order to observe long-range triplet component in the junction superconducting current.

2. Experimental

The LSMO/YBCO bilayers were prepared by in situ pulsed laser deposition (PLD) on $SrTiO_3$ (STO) single crystal substrates. A KrF excimer laser was operating at 248 nm, with a pulse width of 20 ns, repetition rate of 10 Hz and energy density of 6 J/cm^2 (spot size on the target ≈2 mm^2) was used to grow the LSMO and YBCO films. The substrate holder temperature of 850 °C and oxygen pressure of 53 Pa were set during the deposition. After the deposition the films were cooled down at a rate of 20 °C/min in O_2 (4×10^4 Pa). The growth rate of the LSMO as well as the YBCO was about 6.5 nm/min. The thicknesses of LSMO and YBCO layers were 70 nm. To preserve the superconducting and ferromagnetic properties during technological processes the bilayers were covered ex-situ by a 60 nm thick Au film, and then by lift-off deposition of a Ti film of about 60 nm thick. The patterning of the LSMO/YBCO bilayers was at first carried out by argon ion beam etching (IBE) (350 eV, j ≈ 0.1 mA/cm^2) with cooling of the substrate to about −25 °C. In the following step we used Ga^{3+} focused ion beam patterning process. To ensure a homogeneous critical current density distribution, in the cross-section of the superconducting SFS nanojunctions, the width W of the nanostrips was realized to be smaller than the Pearl's penetration depth $\lambda_\wedge = 2\lambda^2/d \approx 700$ nm, where $\lambda \approx 160$ nm is the London penetration depth of the YBCO in a-b plane and $d \approx 70$ nm is the thickness of the YBCO film. The critical temperature and critical current density of the prepared structures were measured by a standard dc four-point method. The SFS nanojunction cross section of the lateral geometry is shown in Fig. 1.

3. Results and discussion

The single thin films of YBCO, LSMO or bilayers LSMO/YBCO prepared on STO substrate exhibit appropriate structural, morphological, electrical and magnetic properties. The X-ray diffractions (θ-2θ scans, ϕ-scans, ω-scans) showed LSMO phase purity, c-axis orientation and high degree of growth epitaxy [10]. The morphology and roughness of the LSMO film surface were investigated by scanning electron microscope (SEM) and atomic force microscope [11]. The LSMO and YBCO films as well as LSMO/YBCO bilayers exhibit very good electrical and magnetic properties (Fig. 2). The resistivity at temperature of T = 100 K is about 250 μΩ cm for the

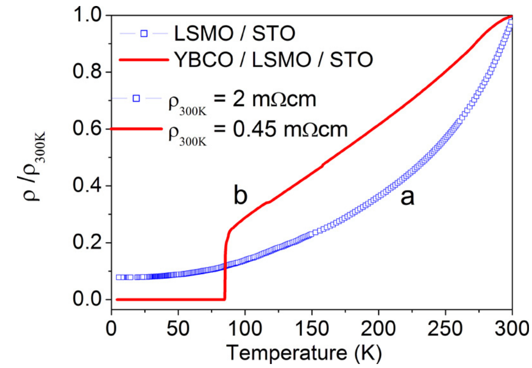

Fig. 2. The normalized resistivity vs. temperature dependence for LSMO film (a) and LSMO/YBCO bilayer (b), both 70 nm thick.

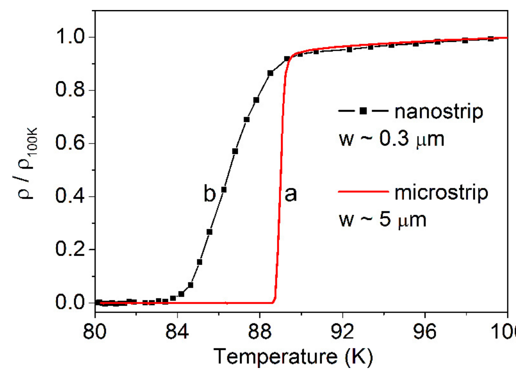

Fig. 3. Superconducting phase transition of 5 μm wide bilayer microstrip (a) and bilayer nanostrip of width w ≈300 nm (b).

LSMO film and 150 μΩ cm for the YBCO films. In temperature range below 80 K, where a working point of SFS nanojunctions is expected, the changes of LSMO resistivity are only very moderate. The Curie temperature T_{Curie} of the LSMO on STO was observed at 412 K and the magnetization vs. temperature dependence indicate nearly 100% spin polarization in the LSMO for temperature below 80 K [10,12].

In Fig. 2 we show ρ(T) dependences of the LSMO film (curve a) and LSMO/YBCO bilayer (curve b), both films are 70 nm thick. The linear dependence of resistivity in temperature range 300–100 K, the zero resistance critical temperature $T_{C0} \approx 89$ K and the width of the superconducting phase transition $\Delta T \approx 0.25$ K were typical for single YBCO films or bilayers. The superconducting transition temperature of bilayer microstrip with the width of w ≈ 5 μm and with YBCO film thickness more than 50 nm remains the same as for single YBCO film because the 50 nm YBCO film thickness is much thicker than the YBCO coherence length ξ_s (Fig. 3, curve a). Subsequent w reduction to nanometer region moderately reduces T_{C0} and enhances the phase transition width (Fig. 3, curve b). The critical current density of the prepared LSMO/YBCO nanostrips, extrapolated to zero temperature was $J_C(0) \approx 10^7$ A/cm^2 which is only one order of magnitude lower than the theoretical Ginzburg-Landau depairing critical current density, indicating high quality of the prepared bilayer structure.

To create the SFS nanojunction of lateral geometry a narrow slot in Ti, Au and YBCO layers of the nanostrip was created by Ga^{3+} FIB perpendicular or parallel to the sample surface. The depth of the slot was chosen to reach the LSMO-YBCO interface. Whereas in the case of perpendicularly incident Ga^{3+} ions the length of the slot L (LSMO length between the YBCO films) was more than 100 nm, in the parallel case the minimal length L we have reached was 40 nm